Environmental Science & Technology

Article

Cite This: Environ. Sci. Technol. 2018, 52, 415−426

pubs.acs.org/est

Urban Organic Aerosol Exposure: Spatial Variations in Composition and Source Impacts

Hugh Z. Li, Timothy R. Dallmann,† Xiang Li, Peishi Gu, and Albert A. Presto*

Center for Atmospheric Particle Studies, Carnegie Mellon University, Pittsburgh, Pennsylvania 15213, United States

Supporting Information

ABSTRACT: We conducted a mobile sampling campaign in a historically industrialized terrain (Pittsburgh, PA) targeting spatial heterogeneity of organic aerosol. Thirty-six sampling sites were chosen based on stratification of traffic, industrial source density, and elevation. We collected organic carbon (OC) on quartz filters, quantified different OC components with thermal-optical analysis, and grouped them based on volatility in decreasing order (OC1, OC2, OC3, OC4, and pyrolyzed carbon (PC)). We compared our ambient OC concentrations (both gas and particle phase) to similar measurements from vehicle dynamometer tests, cooking emissions, biomass burning emissions, and a highway traffic tunnel. OC2 and OC3 loading on ambient filters showed a strong correlation with primary emissions while OC4 and PC were more spatially homogeneous. While we tested our hypothesis of OC2 and OC3 as markers of fresh source exposure for Pittsburgh, the relationship seemed to hold at a national level. Land use regression (LUR) models were developed for the OC fractions, and models had an average R^2 of 0.64 (SD = 0.09). The paper demonstrates that OC2 and OC3 can be useful markers for fresh emissions, OC4 is a secondary OC indicator, and PC represents both biomass burning and secondary aerosol. People with higher OC exposure are likely inhaling more fresh OC2 and OC3, since secondary OC4 and PC varies much less drastically in space or with local primary sources.

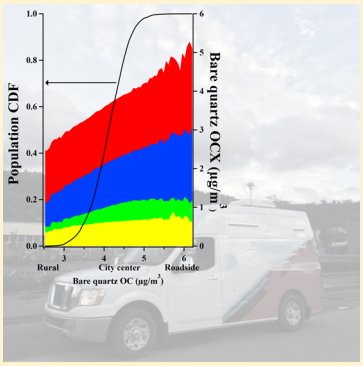

INTRODUCTION

Airborne fine particulate matter ($PM_{2.5}$) continues to pose serious threats to human health, especially to vulnerable groups such as the elderly and children.[1−5] Worldwide, long-term exposure to PM results in 7 million deaths annually.[6] The mechanism how PM exposure reduces life expectancy remains unclear.[3,7] While most air pollution epidemiology studies have focused on the association of health end points with total $PM_{2.5}$ mass,[3,8] evidence suggests that $PM_{2.5}$ compositions may drive some health effects. Epidemiological studies by Krall et al.[9,10] suggest that some PM components and PM from certain sources may be more toxic than others. Compositional differences may also explain the enhanced risks associated with PM exposure in urban versus rural areas.[11] Verma et al.[12] observed that organic aerosol from biomass burning was more effective at generating reactive oxygen species (ROS) than organic aerosol from other sources, suggesting that these emissions may be more toxic. Strak et al.[13] showed that the prevalence of diabetes was related to PM oxidative potential instead of $PM_{2.5}$ mass, suggesting a compositional dependence of human health response. Urch et al.[14] showed strong association of blood pressure increase with particulate organic carbon concentration, but not with total $PM_{2.5}$ mass, as well as a significant negative association between particulate organic carbon and arterial diameter.[15]

Organic carbon (OC) is a major component of PM with a broad range of concentrations from 0.01 to 100 $\mu g/m^3$ worldwide.[16] Ambient OC is a mixture of primary (directly emitted) and secondary (formed via chemical processing) components. Primary organic aerosol such as tailpipe exhaust is semivolatile.[17] Fresh emissions are rapidly diluted in the ambient atmosphere. These emissions partially evaporate to form low-volatility vapors. The photo-oxidation of these newly created vapors, along with photo-oxidation of volatile organic gases, contributes to the burden of secondary ambient organic aerosol.[17] Secondary organic aerosol dominates the OC mass in most environments,[18] however in near source regions (e.g., near roadways) emissions of primary OC can strongly influence population exposures.[19]

National speciation networks, including the Chemical Speciation Network (CSN) and the Interagency Monitoring of Protected Visual Environments (IMPROVE), generally use thermal-optical OC/EC analysis for OC measurements. This method thermally desorbs OC captured by quartz filters at specified temperature ranges in a helium environment.[20] While not chemically specific, the lumped OC fractions evolved at different temperatures—OC1, OC2, OC3, OC4, and pyrolyzed carbon (PC)—are associated with different volatility and may therefore indicate different composition, OC sources, or extents of photochemical processing. Ma et al.[21] found that OC fractions (OCX) are related to volatility, with the most volatile material (OC1) existing almost exclusively in the vapor phase. PC has the lowest volatility and exists almost entirely in the

Received: July 19, 2017
Revised: October 31, 2017
Accepted: December 11, 2017
Published: December 11, 2017

DOI: 10.1021/acs.est.7b03674
Environ. Sci. Technol. 2018, 52, 415−426

particle phase.[21,22] OC2, OC3, and OC4 are more volatile than PC and partition between the particle and vapor phase.

Previous work performed source apportionment of OCX in order to link these OC fractions with specific sources.[23−25] Kim et al.[23] used positive matrix factorization (PMF) to resolve sources for data from a rural IMPROVE site. They found that PC was mostly from a secondary PM factor, and attributed the PC to water-soluble secondary organic carbon produced by oxidation of volatile precursors in the atmosphere. The gasoline factor and diesel factor identified by Kim et al. had high loadings of lower temperature carbon fractions OC2 and OC3. In a separate study, Kim et al.[24] performed PMF analysis for an urban IMPROVE site. The derived diesel factor was rich in OC2. Lee et al.[25] attributed the high OC4 loading in their secondary coal PMF factor to reflect a chemical aging process because the carbon associated with the secondary coal source would have traveled much farther than local traffic emitted OC.

Land use regression (LUR) models are frequently used to estimate population exposures to $PM_{2.5}$ and other air pollutants such as NO_2. LURs link observed concentrations to geographic and land use variables including population density, traffic, and industrial sources. While not a formal source apportionment method, LURs can provide information on different source classes (e.g., traffic) and observed pollutant concentrations.

Many LURs have been built for $PM_{2.5}$ mass concentrations,[26−30] and for PM components such as black carbon and specific PM metals.[26,27,31,32] Few LURs have been built for organic PM constituents. Jedynska et al.[33] built LURs for OC, polycyclic aromatic hydrocarbons (PAHs), and organic molecular markers such as steranes and hopanes in 10 European cities. Hopanes, steranes, and PAHs can all be used as markers for motor vehicle emissions,[34,35] and therefore these LURs could be used to estimate exposures to source-specific PM emissions. We are not aware of other LURs for OC, nor of any LURs built for lumped OC fractions from OC/EC analysis.

In this paper, we present measurements of OC and its thermally resolved fractions using mobile sampling in Pittsburgh and surrounding Allegheny County, PA. The primary objectives of this work are (1) to evaluate intracity spatial variation of OC and its composition, (2) to characterize potential sources of OC fractions, and (3) to derive LUR models of OC and OC fractions for high spatial resolution exposure estimation. We also identify certain OC fractions as indicators of exposure to fresh emissions versus more aged aerosol.

MATERIAL AND METHODS

We chose 36 sites for mobile sampling, which were distributed in Pittsburgh and surrounding cities in Allegheny County, PA. The sampling campaign is described in detail in Li et al.,[26] and the sampling locations are shown in Supporting Information (SI) Figure S1. The landscape is characterized by a plateau with three major river valleys (Allegheny, Monongahela, and Ohio Rivers). A variety of industrial facilities are located along the rivers, such as coke plants, steel manufacturing, and coal-fired electricity stations (SI Figure S1).

Mobile Platform Setup. We used a gasoline powered van, equipped with diverse instruments.[26] Ambient air was pulled by mechanical pumps from a $^1/_2$ in. o.d. stainless steel inlet on top of the van approximately 3 m above ground level.

Ambient air was sampled through a $PM_{2.5}$ cyclone for size selection. Then it was divided into two streams with flow rate controlled at 46 SLPM. We used Teflon filters (47 mm, Teflo R2PJ047, Pall-Gelman) and quartz filters (47 mm, Tissuquartz 2500 QAOUP). One sample line had a Teflon filter in front and a quartz filter behind (QBT, quartz behind Teflon), and the other line had one bare quartz filter (BQ).

Samples were collected with the mobile laboratory parked at curbside. An 8 m hose was connected to the vehicle tailpipe and placed in the downwind direction to avoid self-contamination. Filter sets were also collected from a highway tunnel in Pittsburgh, PA. The sampling configuration in the tunnel is the same as the setup in the mobile van.[36]

Sampling Overview. The sampling strategy is described in detail in Li et al.[26] and Tan et al.[34] Briefly, we selected 36 sites based on three stratification variables−traffic intensity, proximity to major industrial sources, and elevation.[26] The traffic group criteria is annual average daily traffic (AADT) volume obtained from the Pennsylvania Department of Transportation.[37] Locations with AADT > 2800 vehicles/day are classified as high traffic.[26] Proximity to industrial sources takes into account both the distance to the nearest major industrial facility and their emissions. Facilities under consideration have annual $PM_{2.5}$ emissions larger than 50 tons (SI Figure S1). The average distance to the nearest facility for source-impacted sites is about 1500 m. The elevation threshold of 250 m divides sites as either valley (<250 m) or highland (>250 m) according to 2006 Allegheny County, PA contour data.[38] After classification, 19 sites are high traffic density sites, 11 near point sources, and 12 in the valley. SI Table S2 lists the sampling sites and the strata for each site.

We visited sites in two seasons—2013 summer and winter. For each season, we visited every site at three different time sessions on random days—morning (6 a.m. to 12 p.m.), evening (4−10 p.m.), and night (12−5 a.m.).[26] For every sampling session, we parked the van at curbside and sampled for 1 h. Ideally, we would collect 216 quartz filters for each season. We collected 206 out of 216 samples in summer because of pump failures or other errors and all 216 samples in the winter campaign.

We collected 18 tunnel filters in 2013 winter. Sampling is described in detail in Li et al.[36] The sampling time for 14 of the filter sets was 45 min and the remainder were sampled for 90 min. Filters were collected either during midday (12−2 p.m.) or in the afternoon rush hour (3−6 p.m.).

OC Quantification. We use the quartz behind Teflon (QBT) method to correct for sampling artifacts on bare quartz (BQ) filters and to determine particulate OC concentrations.[21,39−41] Two sampling artifacts are involved in this setup: positive and negative artifacts. Positive artifact is when vapors are captured by the bare quartz filter. Negative artifact is when particles are first captured by the filter but then re-evaporate. The BQ filter collects both particle and gas phase OC. The Teflon filter removes the particle phase OC, and the quartz behind Teflon (QBT) filter collects the remaining gas phase OC. The difference between bare quartz OC loading and QBT (BQ-QBT) gives an estimate of the artifact-corrected particle phase OC. In the ambient, there is typically a larger positive artifact than negative artifact, and BQ-QBT approach provides a reasonable artifact-corrected particle phase OC concentration for our sampling setup.[42] Before each sampling session, quartz filters are prebaked in the oven at 550 °C for at least 6 h to remove residual OC.

We used a Sunset OC/EC analyzer (Sunset Laboratories, Inc.) to measure OC concentrations using filter transmittance with the IMPROVE_A protocol.[20] OC desorbs from quartz

DOI: 10.1021/acs.est.7b03674
Environ. Sci. Technol. 2018, 52, 415−426

filters at four different temperature stages in an inert helium environment and are classified as OC1 (<140 °C), OC2 (140−280 °C), OC3 (280−480 °C), and OC4 (480−580 °C). Some OC chars and forms pyrolyzed carbon (PC). PC and elemental carbon (EC) are measured after the carrier gas changes to He/O_2 (O_2: 10%). We used sucrose standards to calibrate the instrument prior to use every time.

We collected approximately 30 field blanks each season. Field blanks went through the same handling procedure as normal samples—filter loading, unloading, and analysis—but no sample was collected. Total carbon loading on all field blanks was lower than 1 $\mu g/cm^2$, which is EPA's standard for clean blank quartz filters.[43] OC on most blanks was lower than the instrument detection limit of 0.2 $\mu g/cm^2$. No blank correction was made because of low signals on field blanks.

The collection area on the quartz filters was 11.34 cm^2. We transformed instrument-reporting values in $\mu g/cm^2$ to ambient concentration in $\mu g/m^3$ by first multiplying by the collection area, and then dividing by the sampling volume. Under typical sampling conditions (46 SLPM for 1 h), the instrument detection limit of 0.2 $\mu g/cm^2$ would be converted to 0.8 $\mu g/m^3$, and measurement resolution would be half the detection limit (0.4 $\mu g/m^3$).[44]

In addition to our data set collected in Pittsburgh, we extracted OC data from the national CSN speciation network.[45] CSN data for OCX and total OC on bare quartz filters were retrieved for 2013.

LUR Model Development. We developed land use regression (LUR) models for OC fractions on bare quartz filters (OC2, OC3, OC4, PC, and total OC). These OC fractions include both particle and gas phase OC. However, quartz filters do not capture all OC vapors with unit efficiency; thus we exclude OC1, which exists almost entirely as vapors in the atmosphere and is poorly captured by quartz filters, from LUR model building.[42,46,47] OCX mentioned afterward in this paper means OC loading on the bare quartz filter. We also derived LUR models for total particle phase OC (BQ-QBT).

LUR is an application of multilinear regression. It associates dependent variables (pollutant concentrations) with multiple independent ones (land use information) using a linear model. Formally, the model format, given p final predictors and n observations at different locations, is

$$y_i = \beta_0 + \beta_1 x_{1i} + \beta_2 x_{2i} + \cdots \beta_p x_{pi} + \varepsilon_i \text{ for } i = 1, 2, \ldots n$$

Following our previous work, the LUR predictor categories are traffic, restaurants, industry, elevation, and other environmental variables.[26] Detailed predictor information is in SI Table S1. In the traffic group, we include variables such as total road length, inverse distance to the nearest road, annual average daily traffic on the nearest road (AADT), bus fuel consumption, and traffic land use zoning area.

The restaurant and industry groups both include point density and inverse distance to the nearest source variables. The industry group also contains inverse distance weighted annual emissions and industrial land use zoning. Other land use variables include commercial and residential land use area, population density, and housing density. Elevation is the altitude of the sampling location above mean sea level.

Since we did not visit all 36 sites at same time on the same day, we need to account for temporal variations that are convolved with our spatially distributed measurements. One approach is to adjust the measured OC by either an additive or multiplicative factor based on measurements at a central reference site.[28,48] An alternative approach is to include the central reference site measurements among the LUR predictor variables.[49] We used the latter approach.

As in our previous LUR study,[26] we use hourly resolved $PM_{2.5}$ measurements at an urban EPA monitoring site (Lawrenceville, SI Figure S1) during concurrent mobile sampling periods as an explanatory variable in our LUR models. Since $PM_{2.5}$ mass concentrations are dominated by secondary species and often regional in nature, variations in $PM_{2.5}$ captured at the central reference site reflect influences of large-scale factors (e.g., weather) that impact the entire sampling domain. The Lawrenceville site was selected as the reference because it represents typical urban background concentrations.

We obtained the road network shapefile from Pennsylvania spatial data access and traffic counts data from Pennsylvania Department of Transportation.[38] We classified roads with annual average daily traffic (AADT) greater than 5000 vehicles per day as major roads. We also define vehicle density (SI Table S1) as the product of AADT and road length.

Locations of restaurants were retrieved from the Allegheny County Health Department. From an air pollution perspective, our primary interest was meat cooking.[50] We therefore excluded restaurants without an obvious cooking source, such as ice cream and coffee shops.

Industry emission and location information came from the National Emission Inventory (2011 NEI).[51] Elevation data were from the USGS National Elevation Data set.[52] Land use type included utility/transport, industrial, commercial, residential, agricultural, or vacant/forest defined by Allegheny County GIS group.[53]

Road and traffic intensity variables were extracted in circular buffers of 25, 50, 100, 300, 500, and 1000 m around each sampling site. The traffic group had the smallest buffer size, starting from 25 m, as traffic related pollutants decrease to background concentrations within 100−500 m of the road edge.[54] The small buffer size indicated the importance of local source emissions. Buffers for land use zoning variables and the restaurant group began with 100 m. The industry group had buffers starting from 1000 m due to transport of pollutants after emission from high stacks.

For LUR model building, we adopted the forward selection approach used by the European Study of Cohorts for Air Pollution Effects (ESCAPE).[28] Potential variables were assigned a prior regression coefficient sign as either positive or negative before they were examined in the variable selection process. The assignment was intuitive, for example, traffic emissions tended to have a positive influence on pollutant concentrations. Thus, traffic related variables would have a positive regression coefficient (β_i) in the model.

In the forward selection process, potential variables were added to the model iteratively. First, univariate regression models were developed for the measured pollutants using individual predictor variables, and the predictor with the highest R^2 was chosen for the initial model. The remaining variables were added to the model separately to create an intermediate model, and adjusted-R^2 was calculated. If the added predictor yielded an increase in adjusted-R^2 greater than 1% and had the same regression coefficient sign as prior assigned, the intermediate model was considered valid and was used as the base model for next round of iteration. This process continued until no more variables could meet the inclusion criteria.

DOI: 10.1021/acs.est.7b03674
Environ. Sci. Technol. 2018, 52, 415−426

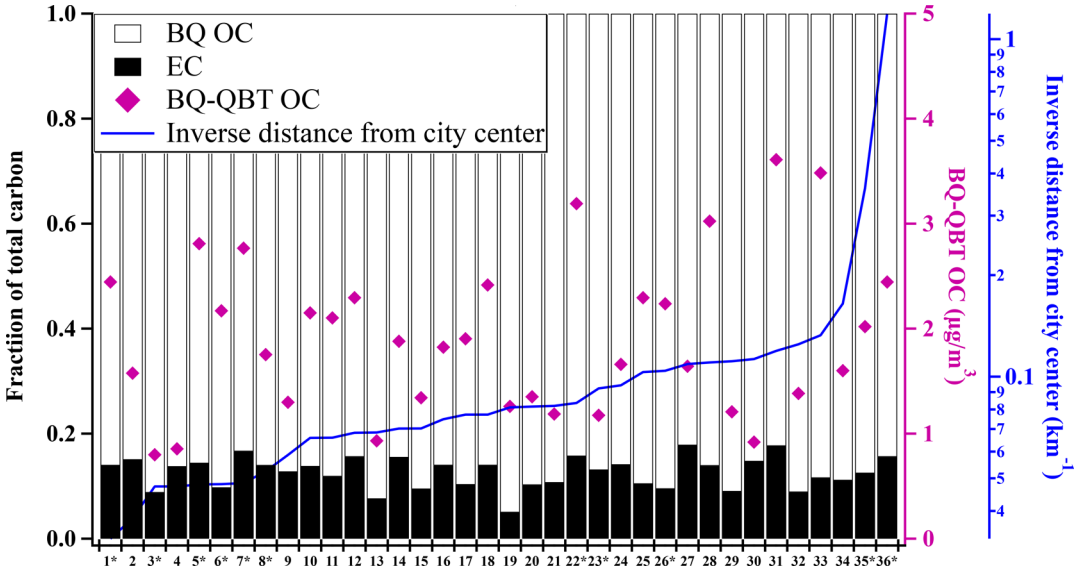

Figure 1. Comparison of quartz filter measurements of average OC and EC at each sampling site. Solid and blank bars indicate relative fractions of total carbon on the left *y* axis. We order the thirty-six sites based on inverse distance from city center, namely from rural to downtown (blue line, log scale on right *y* axis). Sites near point sources are indicated with an asterisk.

We examined the final model for predictor significance, collinearity of predictors, and influential observations (potential outliers). Variables were removed if their *p* values based on an F-test were larger than 0.1 or had a variation inflation factor (VIF) larger than 3. We used Cook's D to signify influential observations. Observations with Cook's D bigger than 1 were further examined by developing and comparing models with this observation or without.

Other model diagnostics included leave-one-out cross validation (LOOCV) R^2, mean studentized prediction residual (MSPR), root-mean-square of studentized residuals (RMS) produced by LOOCV, and Moran's I.[55] LOOCV examined model goodness at predicting test data sets. Each observation was deleted iteratively, and new models were developed using the remaining data. The new model then predicted the deleted observation. Moran's I detected spatial autocorrelation of residuals. LUR, as a linear model, relied on the assumptions that observations were independent of each other. If spatial autocorrelation existed in the final model (*p* value less than 0.05), then this important assumption was violated.

RESULTS AND DISCUSSION

OC Spatial Variation. Figure 1 shows the spatial variation of OC and EC between our 36 sampling sites. Sampling locations are sorted by inverse distance from the city center, and sites near point sources are indicated with an asterisk. The detailed sampling site description is listed in SI Table S2.

Particle phase OC in Pittsburgh[17,21,56] increases from 0.8 $\mu g/m^3$ at urban background and upwind locations to ~4 $\mu g/m^3$ at downtown areas or industrial sites. While BQ-QBT OC (purple symbols in Figure 1) generally increases from rural to urban locations, the increase is not monotonic. This suggests that the spatial variability of particulate OC is multifactorial and does not simply increase along the rural-urban gradient. The highest OC concentrations are typically observed at sites near point sources (mean = 2.25 $\mu g/m^3$).

Overall, OC approximately triples from upwind to near source locations. This spatial variation has important human exposure implications, as OC occupies a large fraction of ambient fine PM. EC is primary in nature and its fraction spans from 4% to 18% of total carbon. The sites with the highest EC fraction are heavily influenced by local industrial emissions and heavy-duty vehicle emissions.[34]

Different Fresh Emission Influence on OCX. Figure 2 shows that the abundance of OCX varies with total OC loading on the bare quartz filter for both ambient and tunnel samples. BQ OC2 has the largest range of concentrations from 0 to 8 $\mu g/m^3$, OC3 from 0 to 6 $\mu g/m^3$, and OC4 and PC tend to be <2 $\mu g/m^3$. Data organize into rows because of the instrument resolution, especially for OC4 and PC. Ambient OC2 and OC3 seem to increase linearly with total OC loading on the bare quartz filter, and concentrations of both are clearly elevated in the tunnel. OC4 also increases with BQ OC, but seems to level off in the ambient samples for BQ OC > ~5−10 $\mu g/m^3$ (though OC4 is slightly elevated in the tunnel relative to ambient). PC levels off in the ambient filters for BQ OC > ~5 $\mu g/m^3$ and is not elevated in the tunnel relative to ambient. The comparison of ambient to tunnel data in Figure 2 suggests that as volatility decreases from OC2 to PC, the contribution of fresh emissions also decreases. The ambient and tunnel data also suggest that primary traffic emissions are not a major source of PC in Pittsburgh.

Figure 2 also compares the ambient and tunnel measurements to published OCX/OC ratios derived from source emissions tests for gasoline and diesel vehicles, cooking, and biomass burning.[57,58] For OC2, all four source relationships describe the ambient and tunnel observations with high R^2 values. This suggests that OC2 is a marker for fresh emissions, but is not source specific.

The observed ambient and tunnel OC3/OC ratios are most similar to diesel emissions (R^2 = 0.7), and gasoline emissions seem to set the lower bound of our Pittsburgh data set. Cooking and biomass burning do not describe the observed OC3 in Pittsburgh. This suggests that OC3 may be a good traffic emissions marker, but it is unclear from our data whether we can definitively claim OC3 as a marker for gasoline or diesel emissions.

DOI: 10.1021/acs.est.7b03674
Environ. Sci. Technol. 2018, 52, 415−426

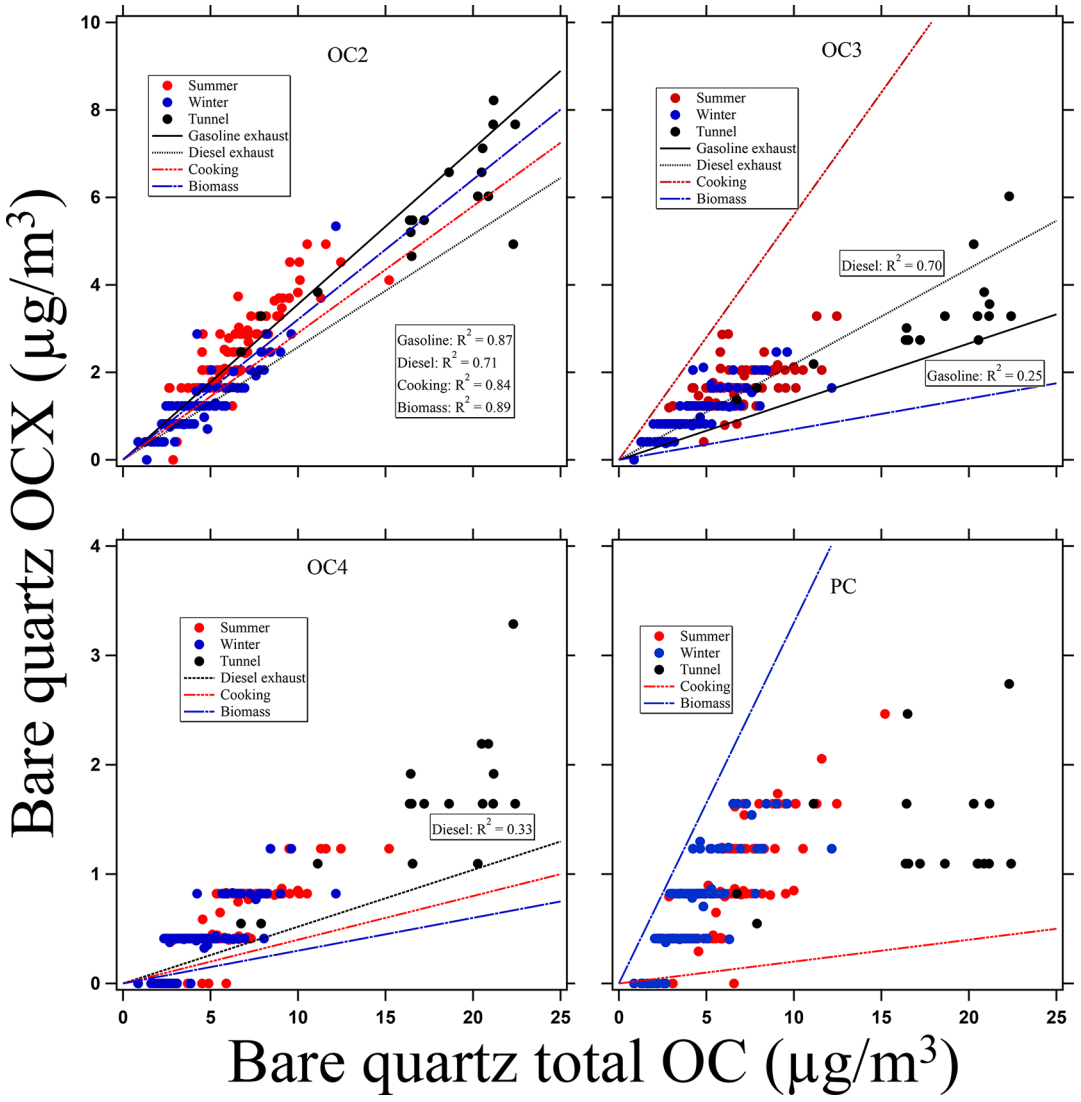

Figure 2. Seasonal comparison of bare quartz OCX on ambient and tunnel filters. Regression lines are from dynamometer studies,[57,58] cooking emission, and biomass burning filters. Diesel, gasoline, cooking and biomass burning lines are all present in OC2 and OC3. OC4 has the diesel, cooking, and biomass lines, and PC has cooking and biomass burning ones. The missing gasoline line in OC4 (and both vehicle lines in PC) results from poor correlation of OC4 (PC) with total OC on source filters. The top and bottom panels have different *y* scales.

Observed ambient and tunnel OC4 are poorly correlated with source test data. Gasoline source tests are omitted from the OC4 panel of Figure 2 because of poor correlation between OC4 and BQ OC. OC4/OC ratios for diesel vehicles, cooking, and biomass burning do not explain the observed ambient and tunnel ratios. The poor correlation between ambient OC4 and the source tests, along with the minimal enhancement of OC4 in the traffic tunnel, suggests that OC4 may be an indicator for secondary organic aerosol.

PC also appears to be a marker of secondary organic aerosol for the Pittsburgh data. This is consistent with charring of ambient secondary OC contributing to measured PC. For example, Yu et al.[59] found that water-soluble OC accounted for a large fraction of charring on quartz filter samples, while hexane extractable organic compounds (nonpolar) produced little charring. The ratio of PC to total water-soluble OC was found to increase with water-soluble OC loading; in other words, the abundance of PC was largely dependent on the fraction of water-soluble secondary OC.

PC was not observed in the gasoline[60,61] and diesel[57,58] exhaust filters shown in Figure 2, but it is observed in wood smoke source tests.[60−62] Figure 2 shows that the PC/OC trend from biomass burning source tests does not describe the Pittsburgh ambient samples, and this is likely because biomass burning is not a major source to $PM_{2.5}$ in Pittsburgh.[63]

Figure 2 suggests that OC2 and OC3 collected on bare quartz filters are good fresh emission markers, with OC3 specifically being a marker for traffic emissions. OC4 and PC are the secondary OC in the study region. The different OCX therefore suggest different source implications.

From Pittsburgh to Nationwide. To broaden study impacts and test our hypothesis of OCX's different fresh emission dependence nationwide instead of just inside the study region, we extracted OC reports from all CSN sites in 2013 and present their relationship with our Pittsburgh data set and source test results in Figure 3.

In Pittsburgh, more volatile OCX (OC2 and OC3) are associated with fresh emissions, and this trend also applies to CSN sites nationwide. The national OC2 data in Figure 3 are

DOI: 10.1021/acs.est.7b03674
Environ. Sci. Technol. 2018, 52, 415−426

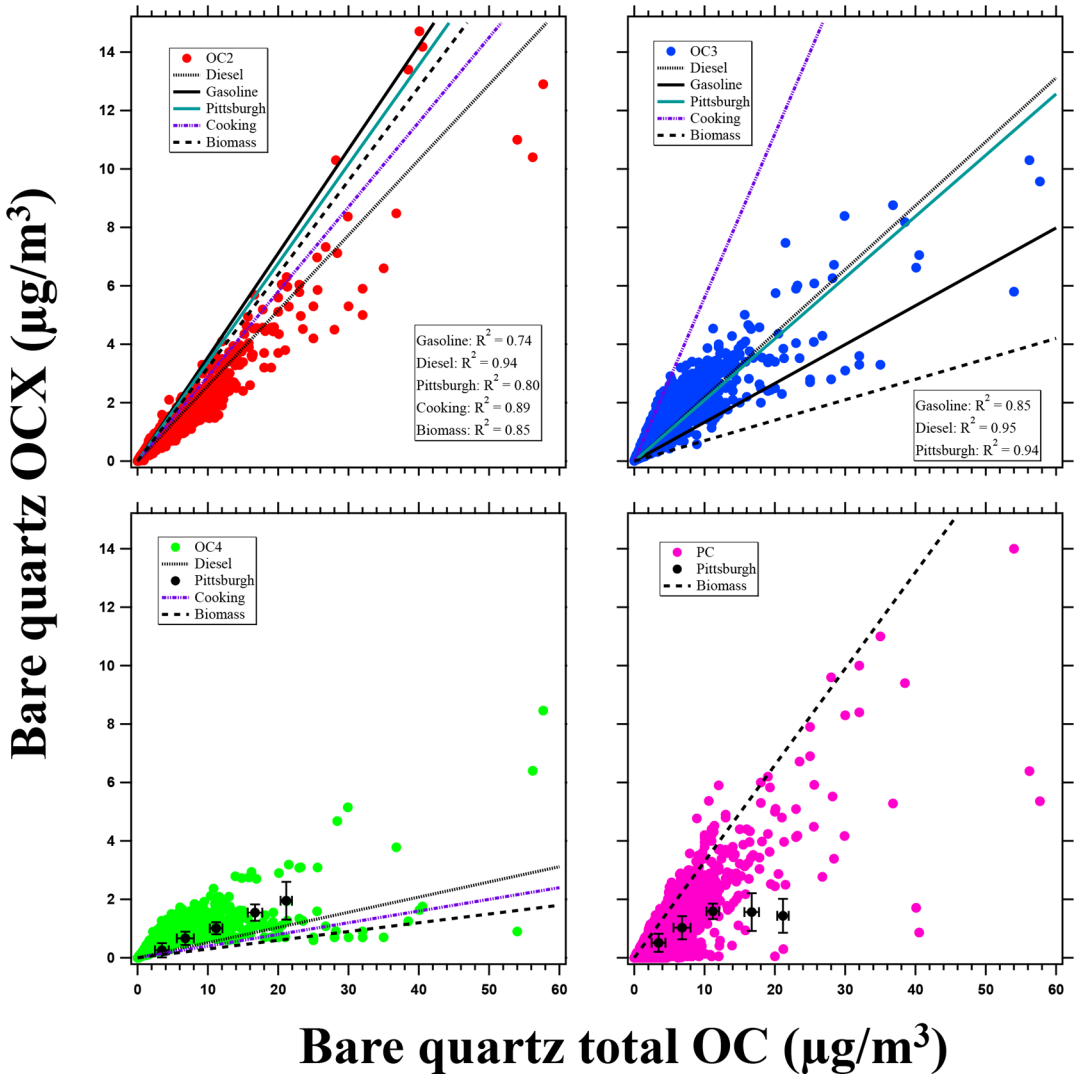

Figure 3. OCX on bare quartz filters from all CSN sites in 2013. Regression lines for Pittsburgh OC2 and OC3 are based on the combined data set of summer, winter, and tunnel. For OC4 and PC, Pittsburgh data are grouped into bins of 2 $\mu g/m^3$, and the error bars show one standard deviation.

linearly correlated with total BQ_OC, and the trend can reasonably be described with OC2/OC ratios from source tests. The Pittsburgh OC2/OC relationship falls along the upper bound of the nationwide OC2 data. The national OC2 data have the strongest agreement with diesel emissions (R^2 = 0.94), whereas for our Pittsburgh data set the strongest agreement was with gasoline vehicles. Nonetheless, the national CSN data suggest that BQ_OC2 is an indicator of fresh emissions, though the specific identify of those emissions may be uncertain.

For OC3, the Pittsburgh and national CSN data largely overlap. Again, agreement is strongest with diesel emissions. Cooking and biomass burning do not describe the observed OC3/OC trend in either the Pittsburgh or national CSN data. Thus, the national CSN data seem to agree with our observation from Figure 2 that OC3 is a marker for traffic emissions.

For OC4 the national data show a similar trend (increasing at low BQ_OC and plateauing at ~1 $\mu g/m^3$ OC4 for BQ_OC > ~ 5−10 $\mu g/m^3$) as the Pittsburgh data and poor agreement with source test results. This again suggests that OC4 may be a marker for secondary organic aerosol.[64,65]

PC is very different between Pittsburgh and the national CSN data. Whereas PC peaks at ~2 $\mu g/m^3$ in Pittsburgh, some CSN sites have much higher PC. Biomass burning is a major source for global/nationwide ambient $PM_{2.5}$ and PC, while it is only a minor source in Pittsburgh.[63,66,67] The implication is that PC in Pittsburgh seems to be an indicator of secondary PM, but in the nationwide data set there seem to be some sites where PC is dominated by biomass burning. These sites fall near the biomass line in Figure 3. Thus, when we consider the Pittsburgh and CSN data together, PC is of mixed origin and interpreting it as either secondary OA or a biomass marker may depend on where the samples are collected, and knowing about sources near sampling sites.

LUR Models. By using mobile sampling measurements (Figure 1) as input, we developed LUR models for bare quartz OC, OC2, OC3, OC4, PC, and particle phase OC (BQ-QBT). The detailed model results are in Table 1. Variable names are briefly described in Table 1 and are described in detail in SI Table S1.

Our LUR models achieve good performance as their R^2 values are all above 0.5.[31,68] Comparison of filter measurements averaged for each of the 36 sampling sites and LUR model predictions at the sampling locations are shown in SI Figure S2. Measurements and predictions generally agree with each other and are distributed along the 1:1 line.

DOI: 10.1021/acs.est.7b03674
Environ. Sci. Technol. 2018, 52, 415−426

Table 1. LUR Model Parameters (β) and Diagnostic Test Results[a]

Model Performance					Model Variables					Model Evaluation		
Species	Quartz source	R^2	Adj usted R^2	LOOCV R^2	Traffic	Industry	Central reference site	Others	Intercept	Moran's I	MSPR	RMS
OC_BQ	BQ	0.76	0.72	0.68	[b]RDALL300 (1.69×10^{-4}) [b]DISTINVALL(3.05) [b]MAJAADT_DIS (2.56×10^{-4})		[b]CSMPM (2.37×10^{-1})	[b]LUVaFo500 (-1.66×10^{-6})	1.39	0.06(0.36)	-5.72×10^{-4}	1.03
OC2	BQ	0.50	0.45	0.38	RAIL500(1.94×10^{-4}) ALLDIESAADT_DIS2 (1.58×10^{-2})		CSMPM (8.97×10^{-2})		5.22×10^{-1}	−0.19(0.11)	-5.31×10^{-4}	1.03
OC3	BQ	0.61	0.56	0.40	RDALL25(4.79×10^{-3}) RAIL50(3.21×10^{-3}) VEHDENSALL500 (1.56×10^{-3})			LUVaFo1000 (-2.01×10^{-7})	1.11	0.04(0.48)	9.29×10^{-3}	1.07
OC4	BQ	0.70	0.64	0.57		[b]PointDe_NEI_PM_Popu_5000 (1.12×10^{-5})	CSMPM (2.16×10^{-2})	POP100 (1.22×10^{-3}) LUCOMM300 (1.84×10^{-6}) LUAGRI1000 (-6.29×10^{-7}) LURES500 (3.25×10^{-7})	-3.77×10^{-2}	0.02(0.62)	1.47×10^{-3}	1.01
PC	BQ	0.60	0.55	0.49	RAIL500(1.65×10^{-4})	PointDe_NEI_PM_1500 (1.61×10^{-1})	CSMPM (5.31×10^{-2})	LURES500 (5.97×10^{-7})	-1.63×10^{-1}	−0.01(0.82)	4.80×10^{-3}	1.02
OC	BQ-QBT	0.71	0.66	0.59	RDALL25(1.06×10^{-2})	PointDe_NEI_All_10000 (4.32)	CSMPM (2.06×10^{-1})	LUINDUS100 (5.02×10^{-5}) LUCOMM1000 (7.07×10^{-7})	−2.00	0.02(0.61)	7.32×10^{-3}	1.05

[a]Values in parentheses are coefficients for final predictors except for those in Moran's I column, which are p values. Elevation and restaurant groups are not included in the table as no final models include these variables. Detailed variable meanings are in SI Table S1. Selected variables ([b]) are explained in the footnote. [b]RDALL300: total road length within surrounding 300 m circular buffers. DISTINVALL: inverse distance to nearest roads. MAJAADT_DIS: nearest major road AADT (annual average daily traffic) times the inverse distance to it. CSMPM: PM measurement at reference site during mobile sampling periods. LUVaFo500: Vacant/Forest land-use areas within surrounding 500 m circular buffers. PointDe_NEI_PM_Popu_5000: PM point sources density in NEI.

DOI: 10.1021/acs.est.7b03674
Environ. Sci. Technol. 2018, 52, 415−426

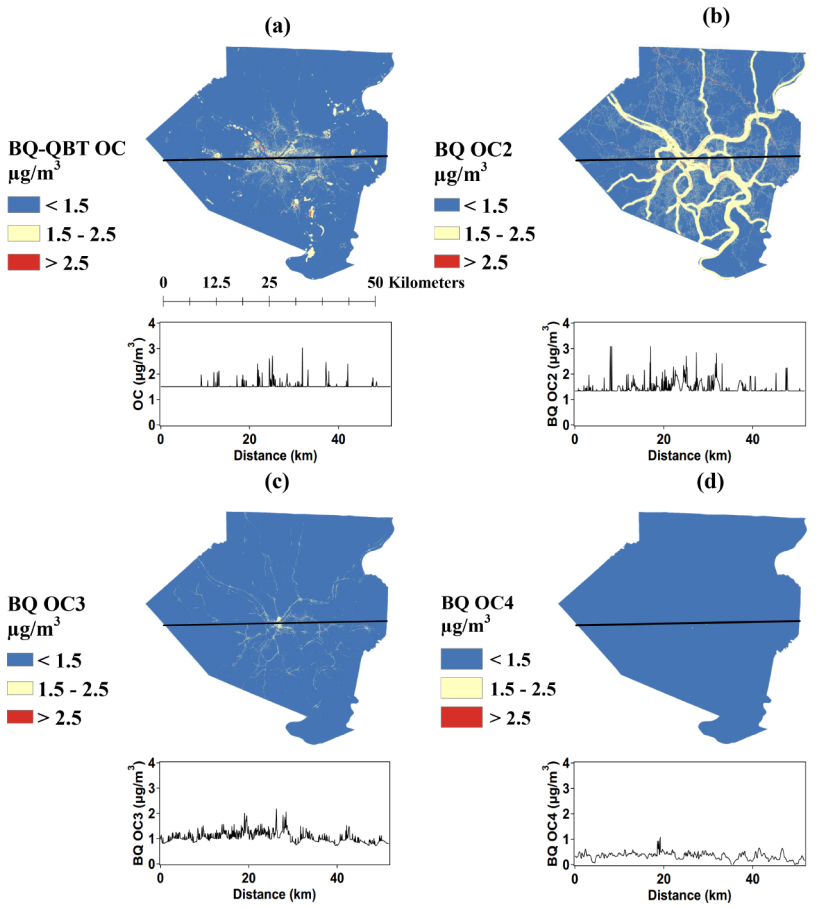

Figure 4. LUR predicted BQ-QBT OC concentration (a), BQ OC2 (b), OC3 (c), and OC4 (d) for the whole study region of Allegheny County, PA. Plots under the maps are the projected pollutant predictions along the black transect lines. The shapefile is downloaded from Pennsylvania Spatial Data Access.[38]

The number of independent predictors in LUR models ranges from 3 to 6. The central reference site group appears in every model except BQ OC3, and this indicates strong association between OC and regional background $PM_{2.5}$ concentrations, as expected.[17] Predictors from the elevation and restaurant groups are not selected in the final models.

As described above, we evaluated LUR models using LOOCV, MSPR, RMS, and Moran's I. A R^2 shrinkage of 0.15 or smaller between original and LOOCV model indicates stable models.[31,68] All derived models are stable. The ideal value for MSPR is 0, and that for RMS is 1. All models have MSPR value close to 0, and the largest RMS is 1.07. We do not detect any spatial autocorrelation of residuals based on Moran's I.

We used the LUR models to generate pollutant prediction maps in ArcGIS-10.3 (ESRI, Redlands, CA) with the spatial analyst tool. Since the LUR model purely extrapolates outside the sampling domain,[31,68] we limit the minimum BQ-QBT OC predictions to be 1.5 $\mu g/m^3$ based on an upwind EPA monitor. Artifact-corrected OC concentrations are elevated in urban and near-source regions in Figure 4(a). Primary emission sources are more concentrated in the city center than in rural regions, and these emissions drive local enhancements in particulate (BQ-QBT) OC.

We retrieved annual average particulate (BQ-QBT) OC concentrations from two regulatory PM speciation monitors (Lawrenceville and Liberty; SI Figure S1). These two sites served as an independent test set to evaluate our LUR model, as they were not included as inputs during the LUR model building process. Our BQ-QBT OC prediction at Lawrenceville is 0.04 $\mu g/m^3$ larger than the monitor measurement. The LUR model under predicted OC by 0.5 $\mu g/m^3$ at Liberty. This under prediction at Liberty was also observed in our LUR $PM_{2.5}$ model in the same study domain, suggesting LUR did not fully capture the spatial gradient induced by a nearby major industrial point source.[26]

BQ OCX exhibit different spatial patterns, as shown in Figure 4. Both OC2 and OC3 show significant spatial variability associated with fresh emissions, primarily from traffic sources. The road network is evident as yellow areas in both Figure 4(b) and (c). OC2 and OC3 are both elevated in the Pittsburgh central business district (center of the map), where there is both high traffic and large emissions from other human activities (e.g., restaurants). On the other hand, the concentration surface of OC4 is less variable in Figure 4(d).

The plot under each LUR map is projected from the black line in the map and quantifies the spatial variation of BQ-QBT OC, BQ OC2, OC3, or OC4 across a transect. BQ-QBT OC increases from 1.5 $\mu g/m^3$ to 2−3 $\mu g/m^3$ on a neighborhood scale (1−2 km) but otherwise is mostly at the background—most of the observed OC is regional. BQ OC2 and OC3 are enhanced near busy roads and the city center. People living near roadways have higher OC2 and OC3 exposures, though since OC2 and OC3 partition between phases, not all of this

DOI: 10.1021/acs.est.7b03674
Environ. Sci. Technol. 2018, 52, 415−426

enhanced OC2 or OC3 shows up in the BQ-QBT map. OC4 is nearly invariant, and oscillates around 0.5 $\mu g/m^3$ across the whole model prediction domain.

Exposure Implications. Figure 2 shows that BQ OC2 has the largest concentration range of the OC fractions in Pittsburgh (0−6 $\mu g/m^3$), whereas OC4 and PC are less variable (0−2 $\mu g/m^3$). OC2 and OC3 seem to be associated with fresh emissions. Higher total BQ and BQ-QBT OC is therefore driven by changes in OC2 and OC3, whereas OC4 and PC are more spatially homogeneous. This means that variations in exposure to total OC mass are convolved with variations in the OC composition.

Figure 5 quantifies this variation and provides an estimate of human exposure considering the spatial heterogeneity of OCX

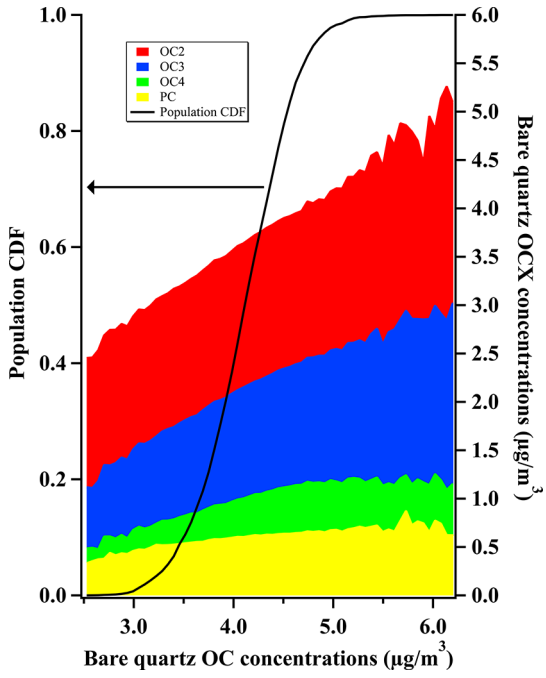

Figure 5. CDF of Population exposure to bare quartz OC (left *y* axis) in Allegheny County, PA. Stacked lines of different color show LUR predicted BQ OCX concentrations (right *y* axis) as a function of total BQ OC concentration.

and varying population density. We first obtained population of every census block in Allegheny county (~30 000 blocks),[69] and assumed the population was evenly distributed in the block. We then assigned a block-averaged LUR OCX prediction to each block.

The black line in Figure 5 shows the cumulative distribution function (CDF) of population-weighted BQ OC exposure. The stacked colors show the distribution of BQ OC among OC2, OC3, OC4, and PC. As noted above, we do not directly consider OC1, which exists almost exclusively as vapor in the atmosphere and is not captured efficiently by quartz filters. Therefore, the sum of OC2, OC3, OC4, and PC (right *y*-axis) is less than the total BQ OC (*x*-axis).

Figure 5 shows that variations in BQ OC exposure are driven almost entirely by the more volatile OC2 and OC3 fractions. For example, population-weighted BQ OC increases from ~3.5 to ~4.5 $\mu g/m^3$ from the 10th to the 90th percentile. OC4 and PC account for approximately 10% of the difference, increasing from ~1 to ~1.1 $\mu g/m^3$, whereas OC2 and OC3 account for the remaining 90% of the additional exposure.

In urban areas with high population and source density, people are exposed to higher BQ OC because of the local enhancement of OC2 and OC3 from primary sources such as traffic and restaurants. On the other hand, the relatively constant concentrations of OC4 and PC indicate that people living in both urban and rural areas are inhaling similar concentrations of secondary OC4 and PC. When people move from rural areas to downtown, exposures to primary OC2 and OC3 increase while those of secondary OC4 and PC are roughly the same. Since OC4 and PC are effectively always in the particle phase,[15] everyone is breathing the spatially homogeneous portion of the (mostly secondary) OC.

Figure 5 shows exposures for BQ OC, and bare quartz filters capture both particulate and vapor-phase organics. We would expect the exposure contrast for particulate (BQ-QBT) OC to be somewhat muted, because OC2 and OC3 are semivolatile, and exist partially as vapors in the atmosphere. Nonetheless, a similar exposure pattern should hold for particulate OC: spatially homogeneous background aerosol (secondary OC4 and PC) punctuated by zones of higher exposure due to local emissions sources.

LIMITATIONS

The major limitation of this paper is the short-duration quartz filter sampling. Tan et al.[70] showed that short-term mobile sampling was less adept at estimating long-term average pollutant concentrations compared with stationary monitors. Nonetheless, our recent study demonstrated that mobile measurements could capture spatial variation of $PM_{2.5}$ and its constituents and were adequate for developing LUR models.[26]

The BQ-QBT method can overcorrect OC artifacts and lead to smaller concentrations.[42] We assume that BQ-QBT works well for artifact correction, and that filters do a good job of capturing particle plus vapors for OC2, OC3, OC4, and PC. This may not be a perfect assumption. However, it is worth noting that our sampling setup is a common one, which makes it easy to compare to data from nationwide networks such as CSN and IMPROVE.

To avoid unrealistic LUR prediction due to model extrapolation, we set a reference standard for our lowest BQ-QBT OC concentration using the upwind EPA Florence site. The Florence site reports bare quartz carbon speciation. We used the volatility basis set framework[71] to calculate particle OC and treated it as the lowest particle OC prediction in our LUR maps.

ASSOCIATED CONTENT

Supporting Information

The Supporting Information is available free of charge on the ACS Publications website at DOI: 10.1021/acs.est.7b03674.

Additional information as noted in text. Map showing 36 sampling locations, comparison of measurements with LUR predictions, tables describing of LUR predictors and site stratification (PDF)

AUTHOR INFORMATION

Corresponding Author

*E-mail: apresto@andrew.cmu.edu.

ORCID

Hugh Z. Li: 0000-0002-1800-8006

DOI: 10.1021/acs.est.7b03674
Environ. Sci. Technol. 2018, 52, 415−426

Present Address

[†]T.R.D.: The International Council on Clean Transportation, Washington, DC 20005, United States.

Notes

The authors declare no competing financial interest.

■ ACKNOWLEDGMENTS

The work was funded by Heinz Endowments grant number E0678, EPA STAR grant number RD83587301, and NSF grant number AGS1543786. We thank Yi Tan at the California Air Source Board for assistance with LUR source data, Sarah Rose Eilenberg at Carnegie Mellon University for biomass filter analysis, and Katerina Liagou at University of Patras for cooking filter results.

■ REFERENCES

(1) Pope, C. A.; Xu, X.; Spengler, J. D.; Ware, J. H.; Fay, M. E.; Ferris, B. G., Jr.; Speizer, F. E. *N. Engl. J. Med.* **1993**, *329* (24), 1753−1759.

(2) Pope, C. A.; Dockery, D. W. Health Effects of Fine Particulate Air Pollution: Lines that Connect. *J. Air Waste Manage. Assoc.* **2006**, *56* (6), 709−742.

(3) Brook, R. D.; Rajagopalan, S.; Pope, C. A.; Brook, J. R.; Bhatnagar, A.; Diez-Roux, A. V.; Holguin, F.; Hong, Y.; Luepker, R. V.; Mittleman, M. A.; et al. Particulate Matter Air Pollution and Cardiovascular Disease: An Update to the Scientific Statement From the American Heart Association. *Circulation* **2010**, *121* (21), 2331−2378.

(4) Di, Q.; Wang, Y.; Zanobetti, A.; Wang, Y.; Koutrakis, P.; Choirat, C.; Dominici, F.; Schwartz, J. D. Air Pollution and Mortality in the Medicare Population. *N. Engl. J. Med.* **2017**, *376* (26), 2513−2522.

(5) Beelen, R.; Raaschou-Nielsen, O.; Stafoggia, M.; Andersen, Z. J.; Weinmayr, G.; Hoffmann, B.; Wolf, K.; Samoli, E.; Fischer, P.; Nieuwenhuijsen, M.; et al. Effects of long-term exposure to air pollution on natural-cause mortality: an analysis of 22 European cohorts within the multicentre ESCAPE project. *Lancet* **2014**, *383* (9919), 785−795.

(6) Brauer, M.; Freedman, G.; Frostad, J.; van Donkelaar, A.; Martin, R. V.; Dentener, F.; Dingenen, R.; van Estep, K.; Amini, H.; Apte, J. S.; et al. Ambient Air Pollution Exposure Estimation for the Global Burden of Disease 2013. *Environ. Sci. Technol.* **2016**, *50* (1), 79−88.

(7) Schwartz, J.; Dockery, D. W.; Neas, L. M. Is daily mortality associated specifically with fine particles? *J. Air Waste Manage. Assoc.* **1996**, *46* (10), 927−939.

(8) Pope, C. A.; Ezzati, M.; Dockery, D. W. Fine-Particulate Air Pollution and Life Expectancy in the United States. *N. Engl. J. Med.* **2009**, *360* (4), 376−386.

(9) Krall, J. R.; Mulholland, J. A.; Russell, A. G.; Balachandran, S.; Winquist, A.; Tolbert, P. E.; Waller, L. A.; Sarnat, S. E. Associations between Source-Specific Fine Particulate Matter and Emergency Department Visits for Respiratory Disease in Four U.S. Cities. *Environ. Health Perspect.* **2017**, *125* (1), 97−103.

(10) Krall, J. R.; Anderson, G. B.; Dominici, F.; Bell, M. L.; Peng, R. D. Short-term Exposure to Particulate Matter Constituents and Mortality in a National Study of U.S. Urban Communities. *Environ. Health Perspect.* **2013**, DOI: 10.1289/ehp.1206185.

(11) Bravo, M. A.; Ebisu, K.; Dominici, F.; Wang, Y.; Peng, R. D.; Bell, M. L. Airborne Fine Particles and Risk of Hospital Admissions for Understudied Populations: Effects by Urbanicity and Short-Term Cumulative Exposures in 708 U.S. Counties. *Environ. Health Perspect.* **2017**, *125* (4), 594−601.

(12) Verma, V.; Fang, T.; Xu, L.; Peltier, R. E.; Russell, A. G.; Ng, N. L.; Weber, R. J. Organic aerosols associated with the generation of reactive oxygen species (ROS) by water-soluble $PM_{2.5}$. *Environ. Sci. Technol.* **2015**, *49* (7), 4646−4656.

(13) Strak, M.; Janssen, N.; Beelen, R.; Schmitz, O.; Vaartjes, I.; Karssenberg, D.; van den Brink, C.; Bots, M. L.; Dijst, M.; Brunekreef, B.; et al. Long-term exposure to particulate matter, NO2 and the oxidative potential of particulates and diabetes prevalence in a large national health survey. *Environ. Int.* **2017**, *108* (SupplementC), 228−236.

(14) Urch, B.; Brook, J. R.; Wasserstein, D.; Wasserstein, D.; Brook, R. D.; Brook, R. D.; Rajagopalan, S.; Corey, P.; Silverman, F. Relative Contributions of PM2.5 Chemical Constituents to Acute Arterial Vasoconstriction in Humans. *Inhalation Toxicol.* **2004**, *16* (6−7), 345−352.

(15) Urch, B.; Silverman, F.; Corey, P.; Brook, J. R.; Lukic, K. Z.; Rajagopalan, S.; Brook, R. D. Acute Blood Pressure Responses in Healthy Adults During Controlled Air Pollution Exposures. *Environ. Health Perspect.* **2005**, *113* (8), 1052−1055.

(16) Jimenez, J. L.; Canagaratna, M. R.; Donahue, N. M.; Prevot, A. S. H.; Zhang, Q.; Kroll, J. H.; DeCarlo, P. F.; Allan, J. D.; Coe, H.; Ng, N. L.; et al. Evolution of Organic Aerosols in the Atmosphere. *Science* **2009**, *326* (5959), 1525−1529.

(17) Robinson, A. L.; Donahue, N. M.; Shrivastava, M. K.; Weitkamp, E. A.; Sage, A. M.; Grieshop, A. P.; Lane, T. E.; Pierce, J. R.; Pandis, S. N. Rethinking Organic Aerosols: Semivolatile Emissions and Photochemical Aging. *Science* **2007**, *315* (5816), 1259−1262.

(18) Zhang, Q.; Jimenez, J. L.; Canagaratna, M. R.; Allan, J. D.; Coe, H.; Ulbrich, I.; Alfarra, M. R.; Takami, A.; Middlebrook, A. M.; Sun, Y. L.; et al. Ubiquity and dominance of oxygenated species in organic aerosols in anthropogenically-influenced Northern Hemisphere midlatitudes. *Geophys. Res. Lett.* **2007**, *34* (13), L13801.

(19) Donahue, N. M.; Posner, L. N.; Westervelt, D. M.; Li, Z.; Shrivastava, M.; Presto, A. A.; Sullivan, R. C.; Adams, P. J.; Pandis, S. N.; Robinson, A. L. Where Did This Particle Come From? Sources of Particle Number and Mass for Human Exposure Estimates. In *Airborne Particulate Matter*; Royal Society of Chemistry: Cambridge, 2016; pp 35−71.

(20) Chow, J. C.; Watson, J. G.; Chen, L.-W. A.; Chang, M. C. O.; Robinson, N. F.; Trimble, D.; Kohl, S. The IMPROVE_A Temperature Protocol for Thermal/Optical Carbon Analysis: Maintaining Consistency with a Long-Term Database. *J. Air Waste Manage. Assoc.* **2007**, *57* (9), 1014−1023.

(21) Ma, J.; Li, X.; Gu, P.; Dallmann, T. R.; Presto, A. A.; Donahue, N. M. Estimating ambient particulate organic carbon concentrations and partitioning using thermal optical measurements and the volatility basis set. *Aerosol Sci. Technol.* **2016**, *50* (6), 638−651.

(22) Zhu, C.-S.; Cao, J.-J.; Tsai, C.-J.; Shen, Z.-X.; Han, Y.-M.; Liu, S.-X.; Zhao, Z.-Z. Comparison and implications of PM2.5 carbon fractions in different environments. *Sci. Total Environ.* **2014**, *466−467* (Supplement C), 203−209.

(23) Kim, E.; Hopke, P. K. Improving source identification of fine particles in a rural northeastern U.S. area utilizing temperature-resolved carbon fractions. *J. Geophys. Res.* **2004**, *109* (D9), D09204.

(24) Kim, E.; Hopke, P. K. Source Apportionment of Fine Particles in Washington, DC, Utilizing Temperature-Resolved Carbon Fractions. *J. Air Waste Manage. Assoc.* **2004**, *54* (7), 773−785.

(25) Lee, P. K. H.; Brook, J. R.; Dabek-Zlotorzynska, E.; Mabury, S. A. Identification of the Major Sources Contributing to PM2.5 Observed in Toronto. *Environ. Sci. Technol.* **2003**, *37* (21), 4831−4840.

(26) Li, H. Z.; Dallmann, T. R.; Gu, P.; Presto, A. A. Application of mobile sampling to investigate spatial variation in fine particle composition. *Atmos. Environ.* **2016**, *142* (Supplement C), 71−82.

(27) Hankey, Steve; Marshall, Julian D. Land use regression models of on-road particulate air pollution (particle number, black carbon, $PM_{2.5}$, particle size) using mobile monitoring. *Environ. Sci. Technol.* **2015**, *49* (15), 9194−9202.

(28) Eeftens, M.; Beelen, R.; de Hoogh, K.; Bellander, T.; Cesaroni, G.; Cirach, M.; Declercq, C.; Dėdelė, A.; Dons, E.; de Nazelle, A.; et al. Development of Land Use Regression Models for PM2.5, PM2.5 Absorbance, PM10 and PMcoarse in 20 European Study Areas; Results of the ESCAPE Project. *Environ. Sci. Technol.* **2012**, *46* (20), 11195−11205.

DOI: 10.1021/acs.est.7b03674
Environ. Sci. Technol. 2018, 52, 415−426

(29) Chen, L.; Shi, M.; Li, S.; Bai, Z.; Wang, Z. Combined use of land use regression and BenMAP for estimating public health benefits of reducing PM2.5 in Tianjin, China. *Atmos. Environ.* **2017**, *152*, 16−23.
(30) Shi, Y.; Lau, K. K.-L.; Ng, E. Developing Street-Level PM2.5 and PM10 Land Use Regression Models in High-Density Hong Kong with Urban Morphological Factors. *Environ. Sci. Technol.* **2016**, *50* (15), 8178−8187.
(31) de Hoogh, K.; Wang, M.; Adam, M.; Badaloni, C.; Beelen, R.; Birk, M.; Cesaroni, G.; Cirach, M.; Declercq, C.; Dėdelė, A.; et al. Development of Land Use Regression Models for Particle Composition in Twenty Study Areas in Europe. *Environ. Sci. Technol.* **2013**, *47* (11), 5778−5786.
(32) Brokamp, C.; Jandarov, R.; Rao, M. B.; LeMasters, G.; Ryan, P. Exposure assessment models for elemental components of particulate matter in an urban environment: A comparison of regression and random forest approaches. *Atmos. Environ.* **2017**, *151*, 1−11.
(33) Jedynska, A.; Hoek, G.; Wang, M.; Eeftens, M.; Cyrys, J.; Keuken, M.; Ampe, C.; Beelen, R.; Cesaroni, G.; Forastiere, F.; et al. Development of Land Use Regression Models for Elemental, Organic Carbon, PAH, and Hopanes/Steranes in 10 ESCAPE/TRANSPHORM European Study Areas. *Environ. Sci. Technol.* **2014**, *48* (24), 14435−14444.
(34) Tan, Y.; Lipsky, E. M.; Saleh, R.; Robinson, A. L.; Presto, A. A. Characterizing the Spatial Variation of Air Pollutants and the Contributions of High Emitting Vehicles in Pittsburgh, PA. *Environ. Sci. Technol.* **2014**, *48* (24), 14186−14194.
(35) Robinson, A. L.; Subramanian, R.; Donahue, N. M.; Rogge, W. F. Source Apportionment of Molecular Markers and Organic Aerosol1. Polycyclic Aromatic Hydrocarbons and Methodology for Data Visualization. *Environ. Sci. Technol.* **2006**, *40* (24), 7803−7810.
(36) Li, X.; Dallmann, T. R.; May, A. A.; Tkacik, D. S.; Lambe, A. T.; Jayne, J. T.; Croteau, P. L.; Presto, A. A. Gas-Particle Partitioning of Vehicle Emitted Primary Organic Aerosol Measured in a Traffic Tunnel. *Environ. Sci. Technol.* **2016**, *50* (22), 12146−12155.
(37) Pennsylvania Spatial Data Access | Data Summary http://www.pasda.psu.edu/uci/DataSummary.aspx?dataset=56 (accessed October 28, 2017).
(38) Pennsylvania Spatial Data Access | Data Summary http://www.pasda.psu.edu/uci/DataSummary.aspx?dataset=1200 (accessed October 28, 2017).
(39) Turpin, B. J.; Huntzicker, J. J.; Hering, S. V. Investigation of organic aerosol sampling artifacts in the los angeles basin. *Atmos. Environ.* **1994**, *28* (19), 3061−3071.
(40) Turpin, B. J.; Saxena, P.; Andrews, E. Measuring and simulating particulate organics in the atmosphere: problems and prospects. *Atmos. Environ.* **2000**, *34* (18), 2983−3013.
(41) Presto, A. A.; Nguyen, N. T.; Ranjan, M.; Reeder, A. J.; Lipsky, E. M.; Hennigan, C. J.; Miracolo, M. A.; Riemer, D. D.; Robinson, A. L. Fine particle and organic vapor emissions from staged tests of an in-use aircraft engine. *Atmos. Environ.* **2011**, *45* (21), 3603−3612.
(42) Subramanian, R.; Khlystov, A. Y.; Cabada, J. C.; Robinson, A. L. Positive and Negative Artifacts in Particulate Organic Carbon Measurements with Denuded and Undenuded Sampler Configurations Special Issue of Aerosol Science and Technology on Findings from the Fine Particulate Matter Supersites Program. *Aerosol Sci. Technol.* **2004**, *38* (sup1), 27−48.
(43) Chow, J. C.; Watson, J. G.; Chen, L.-W. A.; Rice, J.; Frank, N. H. Quantification of PM2.5 organic carbon sampling artifacts in US networks. *Atmos. Chem. Phys.* **2010**, *10* (12), 5223−5239.
(44) Lubin, J. H.; Colt, J. S.; Camann, D.; Davis, S.; Cerhan, J. R.; Severson, R. K.; Bernstein, L.; Hartge, P. Epidemiologic evaluation of measurement data in the presence of detection limits. *Environ. Health Perspect.* **2004**, *112* (17), 1691−1696.
(45) Solomon, P. A.; Crumpler, D.; Flanagan, J. B.; Jayanty, R. K. M.; Rickman, E. E.; McDade, C. E. U.S. National PM2.5 Chemical Speciation Monitoring Networks—CSN and IMPROVE: Description of networks. *J. Air Waste Manage. Assoc.* **2014**, *64* (12), 1410−1438.
(46) Zhao, Y.; Nguyen, N. T.; Presto, A. A.; Hennigan, C. J.; May, A. A.; Robinson, A. L. Intermediate Volatility Organic Compound Emissions from On-Road Gasoline Vehicles and Small Off-Road Gasoline Engines. *Environ. Sci. Technol.* **2016**, *50* (8), 4554−4563.
(47) Zhao, Y.; Nguyen, N. T.; Presto, A. A.; Hennigan, C. J.; May, A. A.; Robinson, A. L. Intermediate Volatility Organic Compound Emissions from On-Road Diesel Vehicles: Chemical Composition, Emission Factors, and Estimated Secondary Organic Aerosol Production. *Environ. Sci. Technol.* **2015**, *49* (19), 11516−11526.
(48) Wang, M.; Beelen, R.; Basagana, X.; Becker, T.; Cesaroni, G.; de Hoogh, K.; Dedele, A.; Declercq, C.; Dimakopoulou, K.; Eeftens, M.; et al. Evaluation of land use regression models for NO2 and particulate matter in 20 European study areas: the ESCAPE project. *Environ. Sci. Technol.* **2013**, *47* (9), 4357−4364.
(49) Saraswat, A.; Apte, J. S.; Kandlikar, M.; Brauer, M.; Henderson, S. B.; Marshall, J. D. Spatiotemporal Land Use Regression Models of Fine, Ultrafine, and Black Carbon Particulate Matter in New Delhi, India. *Environ. Sci. Technol.* **2013**, *47* (22), 12903−12911.
(50) Schauer, J. J.; Kleeman, M. J.; Cass, G. R.; Simoneit, B. R. T. Measurement of Emissions from Air Pollution Sources. 1. C1 through C29 Organic Compounds from Meat Charbroiling. *Environ. Sci. Technol.* **1999**, *33* (10), 1566−1577.
(51) USEPA. 2011 National Emissions Inventory (NEI) Data https://www.epa.gov/air-emissions-inventories/2011-national-emissions-inventory-nei-data (accessed October 28, 2017).
(52) The National Map: Elevation https://nationalmap.gov/elevation.html (accessed October 28, 2017).
(53) Tan, Y.; Dallmann, T. R.; Robinson, A. L.; Presto, A. A. Application of plume analysis to build land use regression models from mobile sampling to improve model transferability. *Atmos. Environ.* **2016**, *134* (Supplement C), 51−60.
(54) Karner, A. A.; Eisinger, D. S.; Niemeier, D. A. Near-Roadway Air Quality: Synthesizing the Findings from Real-World Data. *Environ. Sci. Technol.* **2010**, *44* (14), 5334−5344.
(55) Mukerjee, S.; Smith, L. A.; Johnson, M. M.; Neas, L. M.; Stallings, C. A. Spatial analysis and land use regression of VOCs and NO2 from school-based urban air monitoring in Detroit/Dearborn, USA. *Sci. Total Environ.* **2009**, *407* (16), 4642−4651.
(56) Subramanian, R.; Donahue, N. M.; Bernardo-Bricker, A.; Rogge, W. F.; Robinson, A. L. Insights into the primary−secondary and regional−local contributions to organic aerosol and PM2.5 mass in Pittsburgh, Pennsylvania. *Atmos. Environ.* **2007**, *41* (35), 7414−7433.
(57) May, A. A.; Presto, A. A.; Hennigan, C. J.; Nguyen, N. T.; Gordon, T. D.; Robinson, A. L. Gas-particle partitioning of primary organic aerosol emissions: (1) Gasoline vehicle exhaust. *Atmos. Environ.* **2013**, *77* (SupplementC), 128−139.
(58) May, A. A.; Presto, A. A.; Hennigan, C. J.; Nguyen, N. T.; Gordon, T. D.; Robinson, A. L. Gas-Particle Partitioning of Primary Organic Aerosol Emissions: (2) Diesel Vehicles. *Environ. Sci. Technol.* **2013**, *47* (15), 8288−8296.
(59) Yu, J. Z.; Xu, J.; Yang, H. Charring Characteristics of Atmospheric Organic Particulate Matter in Thermal Analysis. *Environ. Sci. Technol.* **2002**, *36* (4), 754−761.
(60) Schauer, J. J.; Mader, B. T.; DeMinter, J. T.; Heidemann, G.; Bae, M. S.; Seinfeld, J. H.; Flagan, R. C.; Cary, R. A.; Smith, D.; Huebert, B. J.; et al. ACE-Asia Intercomparison of a Thermal-Optical Method for the Determination of Particle-Phase Organic and Elemental Carbon. *Environ. Sci. Technol.* **2003**, *37* (5), 993−1001.
(61) Chow, J. C.; Watson, J. G.; Crow, D.; Lowenthal, D. H.; Merrifield, T. Comparison of IMPROVE and NIOSH Carbon Measurements. *Aerosol Sci. Technol.* **2001**, *34* (1), 23−34.
(62) Li, X.; Chen, Y.; Bond, T. C. Light absorption of organic aerosol from pyrolysis of corn stalk. *Atmos. Environ.* **2016**, *144*, 249−256.
(63) Robinson, A. L.; Subramanian, R.; Donahue, N. M.; Bernardo-Bricker, A.; Rogge, W. F. Source Apportionment of Molecular Markers and Organic Aerosol. 2. Biomass Smoke. *Environ. Sci. Technol.* **2006**, *40* (24), 7811−7819.
(64) Leskinen, A. P.; Jokiniemi, J. K.; Lehtinen, K. E. J. Characterization of aging wood chip combustion aerosol in an environmental chamber. *Atmos. Environ.* **2007**, *41* (17), 3713−3721.

DOI: 10.1021/acs.est.7b03674
Environ. Sci. Technol. 2018, 52, 415−426

(65) Leskinen, A. P.; Jokiniemi, J. K.; Lehtinen, K. E. J. Transformation of diesel engine exhaust in an environmental chamber. *Atmos. Environ.* **2007**, *41* (39), 8865−8873.
(66) Zhou, Y.; Xing, X.; Lang, J.; Chen, D.; Cheng, S.; Wei, L.; Wei, X.; Liu, C. A comprehensive biomass burning emission inventory with high spatial and temporal resolution in China. *Atmos. Chem. Phys.* **2017**, *17* (4), 2839−2864.
(67) Zhou, S.; Collier, S.; Jaffe, D. A.; Briggs, N. L.; Hee, J.; Sedlacek, A. J., III; Kleinman, L.; Onasch, T. B.; Zhang, Q. Regional influence of wildfires on aerosol chemistry in the western US and insights into atmospheric aging of biomass burning organic aerosol. *Atmos. Chem. Phys.* **2017**, *17* (3), 2477−2493.
(68) Zhang, J. J. Y.; Sun, L.; Barrett, O.; Bertazzon, S.; Underwood, F. E.; Johnson, M. Development of land-use regression models for metals associated with airborne particulate matter in a North American city. *Atmos. Environ.* **2015**, *106* (Supplement C), 165−177.
(69) Geography, U. C. B. 2010 Census - Census Tract Reference Maps https://www.census.gov/geo/maps-data/maps/2010tract.html (accessed October 28, 2017).
(70) Tan, Y.; Robinson, A. L.; Presto, A. A. Quantifying uncertainties in pollutant mapping studies using the Monte Carlo method. *Atmos. Environ.* **2014**, *99* (Supplement C), 333−340.
(71) Donahue, N. M.; Robinson, A. L.; Stanier, C. O.; Pandis, S. N. Coupled Partitioning, Dilution, and Chemical Aging of Semivolatile Organics. *Environ. Sci. Technol.* **2006**, *40* (8), 2635−2643.

DOI: 10.1021/acs.est.7b03674
Environ. Sci. Technol. 2018, 52, 415−426